

A nanosecond-duration radio pulse originating from the defunct Relay 2 satellite

C. W. JAMES ^{1,*} A. T. DELLER ² T. DIAL ² M. GLOWACKI ^{1,3,4} S. J. TINGAY ¹ K. W. BANNISTER ^{5,6} A. BERA ¹
N. D. R. BHAT ¹ R. D. EKERS ^{5,1} V. GUPTA ⁵ A. JAINI ⁷ J. MORGAN ⁸ J. N. JAHNS-SCHINDLER ^{7,9}
R. M. SHANNON ^{7,9} M. SUKHOV ¹⁰ J. TUTHILL ⁵ AND Z. WANG ¹

¹International Centre for Radio Astronomy Research (ICRAR), Curtin University, Bentley, WA 6102, Australia

²Centre for Astrophysics and Supercomputing, Swinburne University of Technology, John St., Hawthorn, VIC 3122, Australia

³Institute for Astronomy, University of Edinburgh, Royal Observatory, Edinburgh, EH9 3HJ, United Kingdom

⁴Inter-University Institute for Data Intensive Astronomy, Department of Astronomy, University of Cape Town, Cape Town, South Africa

⁵Australia Telescope National Facility, CSIRO, Space and Astronomy, PO Box 76, Epping, NSW 1710, Australia

⁶Sydney Institute for Astronomy, School of Physics, University of Sydney, NSW 2006, Australia

⁷Centre for Astrophysics and Supercomputing, Swinburne University of Technology, Hawthorn, VIC 3122, Australia

⁸CSIRO Space and Astronomy, P.O. Box 1130, Bentley, WA 6102, Australia

⁹ARC Centre of Excellence for Gravitational Wave Discovery (OzGrav), Hawthorn, VIC 3122, Australia

¹⁰School of Science, Royal Melbourne Institute of Technology, Melbourne, VIC, 3000

ABSTRACT

We report the detection of a burst of emission over a 695.5 MHz–1031.5 MHz bandwidth by the Australian Square Kilometre Array Pathfinder, ASKAP. The burst was localised through analysis of near-field time delays to the long-decommissioned Relay 2 satellite, and exhibited a dispersion measure of $2.26 \cdot 10^{-5} \text{ pc cm}^{-3}$ — 69.7 TECU, consistent with expectations for a single pass through the ionosphere. After coherent dedispersion, the burst was determined to be less than 30 ns in width, with an average flux density of at least 300 kJy. We consider an electrostatic discharge (ESD) or plasma discharge following a micrometeoroid impact to be plausible explanations for the burst. ESDs have previously been observed with the Arecibo radio telescope, but on 1000 times longer timescales. Our observation opens new possibilities for the remote sensing of ESD, which poses a serious threat to spacecraft, and reveals a new source of false events for observations of astrophysical transients.

Keywords: Time domain astronomy (2109) — Radio transient sources (2008) — Artificial satellites(68)

1. Introduction

The charging of spacecraft in orbit due to interactions with the space environment has been a well-known phenomena since the early days of the space program (DeForest 1972). Accumulation of electrons and ions can lead to large voltage differentials between spacecraft surfaces, and between the spacecraft and space plasmas. Sudden ESD in the form of arc currents can cause damage to spacecraft systems, and although decades of experience has led to design recommendations to avoid this (Garrett & Whittlesey 2012), spacecraft charging remains a hazard. A recent likely example is the temporary loss of the Galaxy 15 satellite in April 2010 (Allen 2010), while numerous, minor discharges have been proposed for the gradual degradation of solar arrays supplying power to GPS satellites (Ferguson et al. 2016). Despite this, most spacecraft do not contain mechanisms for moni-

toring the build-up of charge, or detecting sudden discharges, and the primary method of detection remains the study of the damage caused by ESD (e.g. Leach & Alexander 1995).

The remote sensing of ESD by low-frequency ground-based radio monitors has been proposed as a method to study this phenomena (Ferguson et al. 2014). Strong \sim MHz radio bursts with durations of microseconds have been observed in laboratory experiments aimed at reproducing ESD from the charging of solar arrays (Leung 1985), and recent observations with the Arecibo telescope have detected 300–350 MHz emission typically lasting 40–50 μ s from GPS satellites (Ferguson et al. 2017). However, there has been no systematic campaign capable of observing large numbers of spacecraft.

It has also been proposed that the energetic plasmas produced by high-velocity micrometeoroid impacts with spacecraft may produce radio-frequency emission (Garrett & Close 2013). However, like ESD, literature expectations for this emission suggests durations of at least several μ s, and

* E-mail: clancy.james@curtin.edu.au

emission peaked at low MHz or kHz frequencies (Li et al. 2023).

Here we report the serendipitous detection of a 30 ns duration, 300 kJy impulse from the decommissioned Relay 2 satellite by the Australian Square Kilometre Array Pathfinder (ASKAP; Hotan et al. 2021), which challenges expectations for both ESD and micrometeoroid origins.

We discuss the signal in §2, the origin in the Relay 2 satellite in §3, and the implications for both remote sensing of ESD, and false event rates for astroparticle experiments studying nanosecond radio pulses, in §4.

2. Detection

The burst was detected on 2024 June 13th at 05:13:09.035 UTC (i.e., MJD 60474.21746568846) by ASKAP using the Commensal Realtime ASKAP Fast Transients Survey (CRAFT) coherent detection system, CRACO (Wang et al. 2024). The CRACO system uses aperture synthesis techniques to form total intensity (Stokes I) images in near-real-time, using data from 760.5 MHz to 1000.5 MHz, in 1 MHz channels, at 13.8 ms resolution. ASKAP uses phased-array feed technology to form 36 contiguous images on the sky, each of which are processed separately in parallel by the real-time CRACO system. The burst was detected in beam 17 of ASKAP’s 36 beams with a signal-to-noise ratio of 16.3 at a time resolution of 13.8 ms, with no discernible dispersion in frequency.

Most FRB detection pipelines — including earlier FRB searches performed by ASKAP (Shannon et al. 2024) — routinely reject signals with low dispersion measure due to the prevalence of transient radio-frequency interference (RFI). However, the coherent imaging used by the ASKAP/CRACO system has much stronger terrestrial RFI rejection; terrestrial RFI has a very significantly curved wavefront across the array and will not form a point-source in the image plane, unlike a far-field astrophysical source, facilitating the identification and removal of candidates generated by it. We were additionally motivated to search for undispersed bursts because Galactic objects such as rotating radio transients and long-period transients are detectable by the CRACO system (Wang et al. 2024), and may appear undispersed at our time-resolution of 13.8 ms if they have a DM of $\lesssim 10 \text{ pc cm}^{-3}$.

Our detection triggered a download of 12 s of voltage data (which represents the electric field as sampled by each ASKAP antenna) surrounding the event, for a band from 695.5 MHz to 1031.5 MHz in complex-valued 1 MHz subbands. The raw voltage data saved in this fashion have been quantised with 1-bit precision prior to storage in the buffer, to provide a buffer of useful time length given the available memory; the real-time CRACO detection system makes use of the data prior to this re-quantisation stage, which has much

higher bit depth. The downloaded voltage data were then run through ASKAP’s offline processing pipeline (CELEBI; Scott et al. 2023) to localise the burst.

Iterative offline processing revealed that only antennas within the inner 1 km of ASKAP produced a coherent image under the usual assumption of a far-field source whose wavefronts are planar as they pass the telescope array. Using this sub-set of the array, we recovered a point-like source with apparent position RA=1h34m35.6s \pm 8.1s, DEC=-10°24’27.6" \pm 3.7". As longer baseline data was included, the source S/N progressively reduced. This is indicative of an origin within the near-field limit of ASKAP, which is $2D^2\lambda^{-1} \sim 200,000 \text{ km}$ for the full ASKAP baseline of $D = 6 \text{ km}$, but only 5700 km for $D = 1 \text{ km}$. The burst was unresolved at the standard minimum CELEBI processing timescale of 1 μ s. These characteristics initiated a dedicated analysis chain for this event.

To determine the event characteristics, we first measured the propagation delay between every antenna pair (baseline) independently. To do so, we made use of the far-field calibrated X- and Y- polarisation data produced by the CELEBI pipeline (that are normally used to form a "tied" beam for the purpose of studying burst structure at high time and frequency resolution. Compared to the raw voltages recorded by the ASKAP antennas, these data were gain and polarisation calibrated, and phase-offset relative to a far-field planar wavefront from the apparent source position. Additionally, artefacts due to ASKAP’s over-sampled polyphase filterbank were corrected. These signals were first Fourier transformed to the time domain using a complex-to-complex inverse FFT, giving data at $1/336 \mu\text{s} \sim 3 \text{ ns}$ resolution. This revealed a raw burst duration of approximately 200 ns on 19 of the 22 antennas — the burst was not present on three antennas, likely due to data corruption. Data from these 19 antennas were cropped about the burst and correlated with antenna ak06 to extract a relative arrival time. This revealed time delays of up to 3.4 ns on baselines over 3 km perpendicular to the arrival direction. The arrival times were then fit with a quadratic delay, with time offset scaling as the square of the projected transverse distance about the array centre. A best-fit near-field distance of 4500 km was obtained (see Figure 1), with rms residuals of 0.075 ns. An uncertainty of 80 km was determined by adding rms errors of 0.075 ns to the time-delay data, and re-fitting for the distance.

2.1. Event properties

The identification of a near-field origin allowed CELEBI to be re-run using the delay model derived above. Hence, all burst properties reported below are derived from coherently adding all antennas to form the highest possible S/N beam. A dispersion search was applied to this data, maximising $\sum |dI/dt|^2$. No low-pass filter was applied, as is

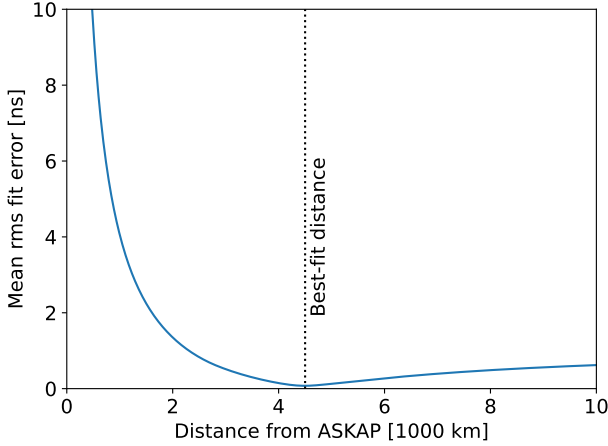


Figure 1. The best-fitting nearfield distance. Shown is the rms of the timing residuals over all 19 antennas used in the fit. The minimum at 4500 km corresponds to the best-fit distance for the burst.

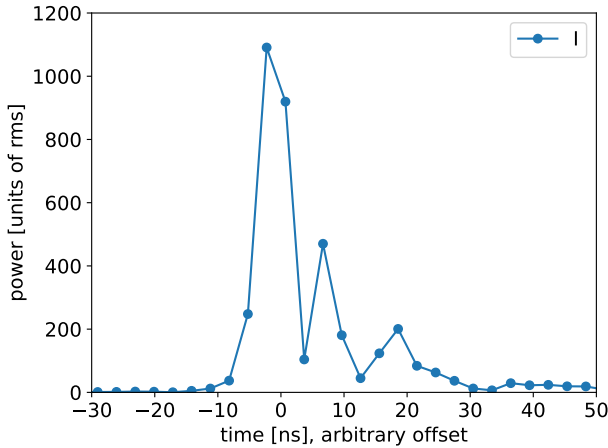


Figure 2. The dedispersed burst. Total burst power at Nyquist resolution (points — lines to guide the eye only) after dedispersion and coherent addition over 19 antennas according to the nearfield fit. Note that our ability to determine the signal flux density — and potentially also shape — is limited by our 1-bit sampling precision (see text).

usually the case (Sutinjo et al. 2023), since structure was observed at the highest time resolution. This produced a best-fit dispersion measure of $2.26 \cdot 10^{-5} \text{ pc cm}^{-3}$, corresponding to 69.7 TECU (total electron content units). This agrees closely with the estimated value of slant total electron content (STEC) of 66 ± 7 TECU using different ionospheric models within the TECOR package in AIPS (Greisen 2003), and 58.9 TECU derived from an ionex map provided by the Centre for Orbit Determination in Europe using the ionFR package (Sotomayor-Beltran et al. 2013).

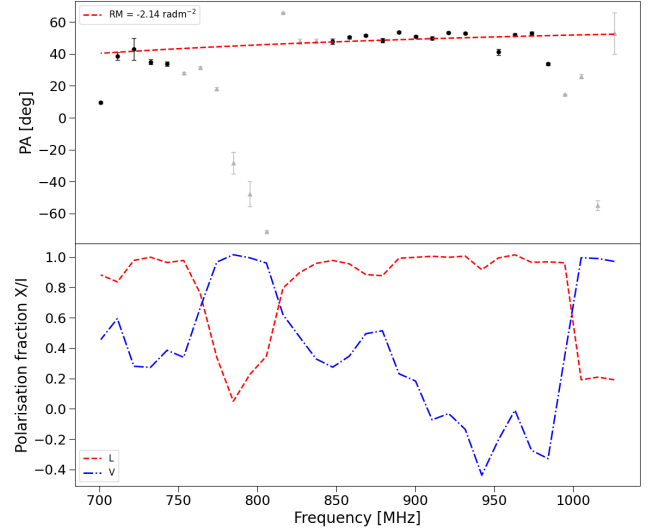


Figure 3. Polarisation properties of the burst. Upper panel: rotation measure (RM) fit to the position angle (PA) of the linear polarisation (black circles) as a function of frequency, with channels not used in the fit shown in grey. Lower panel: the fractional linear (L) and circular (V) polarisations as a function of frequency. Calculations were performed at 10.5 MHz, 95.24 ns resolution.

Coherently de-dispersing the burst at this DM allowed the intrinsic burst structure to be determined. The burst, plotted in Figure 2, consists of a primary impulse of 10 ns duration, with subsequent lower-intensity structure of total duration 30 ns (given our time resolution of 3 ns, we cannot distinguish between a sequence of pulses of decreasing amplitude, versus a single pulse with an oscillating exponential decay). The peak power is 1090 times the off-pulse mean. While this corresponds to a peak power of 112 kJy given ASKAP’s single-dish spectral-equivalent flux density of 1950 Jy at our frequencies (Hotan et al. 2021), this approximately corresponds to the limit of our dynamic range given the one-bit sampling of our buffered data. Indeed, the CRACO S/N trigger (which operates on 8-bit sampling) implies a 30 ns average flux density of 300 kJy, which itself may be at the limit of the dynamic range of the ASKAP system to an impulsive event. Hence, we suspect that the primary pulse is a bandwidth-limited impulse of true duration 3 ns or less and peak flux density of 3 MJy or more. Assuming the 3 MJy value over our 336 MHz bandwidth gives an incident power of $10^{-11} \text{ W m}^{-2}$. At a distance of 4500 km, this corresponds to a source electric field strength of 280 V m^{-1} ; assuming 2 sr of emission from a surface (see §3), this implies a peak power output of 400 W (energy of $1.2 \mu\text{J}$ and assuming a 3 ns intrinsic duration).

We determine the rotation measure (RM) of the event to be -2.14 rad m^{-2} — smaller in magnitude than, but comparable to, a value of -3.0 rad m^{-2} expected from our ionospheric modelling. De-rotating the event allows us to determine its

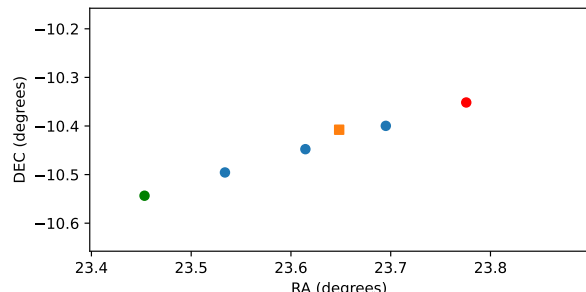


Figure 4. The match of the observed burst position and the Relay 2 position The orange square marker is the observed burst position. The blue markers are positions of Relay 2, with green and red markers indicating first and last time points, respectively, separated by one second and centred on the observed burst time.

full polarisation properties, as shown in Figure 3. At most frequencies, it is purely linearly polarised, but shifts to being 100% circularly polarised at two specific parts of the band, near 800 MHz and 1 GHz. Since polarisation properties are changing at inverse bandwidth resolution, our analysis forces the total polarisation fraction to be 100% — when polarisation properties are averaged over the burst, it is 75% polarised.

3. Origin of the burst

The 4500 km distance to the burst suggests an Earth satellite as the origin. Using the location of ASKAP, the time of the burst, and the Skyfield python module¹, we searched for a coincidence in time and position on the sky between the burst and Earth satellites. The Two Line Element (TLE) descriptions of Earth satellite orbital parameters were downloaded from the space-track.org catalog, for all satellites in the catalog and for dates two days either side of the observation time. Skyfield was used to propagate the orbital parameters to the observation time and calculate the Right Ascension and Declination for each satellite, as seen from the location of ASKAP. One viable match was found, for NORAD ID 737 (Relay 2).² Relay 2 was seen to be within 3.2' of the observed burst position at the observation time. Skyfield also calculates the distance between ASKAP and Relay 2 at 4322 km at the observation time — reasonably consistent with the estimated distance of 4500 km \pm 80 km. An angular distance of 3.2' corresponds to 4 km in the plane of the sky at a distance of 4322 km. Figure 4 shows the position on the sky, as seen from ASKAP, of the observed burst location and Relay 2 in a five-second window centred on the observed burst

time. We therefore conclude that this burst originated with Relay 2.

The Relay 2 satellite was launched by NASA on 1964 Jan. 21, on an elliptical orbit with perigee 2091 km, apogee 7411 km, and inclination 46.3°.³ It was primarily a telecommunications satellite, with uplink frequencies between 1723.33 and 1726.67 MHz, and downlink frequencies from 4164.72 MHz to 4174.72 MHz (Goddard Space Flight Centre 1965). It contained two transponders, both of which had ceased to function by 1967 June 9. It also carried three particle detection experiments — a set of proton-electron detectors, a radiation damage experiment, and a solid-state ion chamber — designed to study the inner Van Allen radiation belt. A comprehensive final report on the virtually identical RELAY 1 mission can be found at <https://ntrs.nasa.gov/citations/19660000937>.

Operations of Relay 2 ceased on September 26, 1965 (NASA Historical Staff, Office of Policy Analysis 1966). We therefore rule out that the burst was a deliberate transmission. While re-commencement of transmissions by defunct satellites has been observed⁴, a 30 ns pulse does not naturally correspond to any on-board system.

We have searched 0.5 s of data about this signal for additional sub-pulses, and find the peak power to be only 6.5 standard deviations above the mean, consistent with random fluctuations. Since we have not yet verified the nearfield tracking of objects in our search pipeline, as few as five of the innermost antennas would coherently detect the moving satellite over the full 0.5 s. Nonetheless, this corresponds to a limit of 2500 Jy on associated bursts from Relay 2.

In 13.8 ms mode, CRACO has observed for 100.5 days between 2024 May 6th and 2025 Feb. 19th, during which Relay 2 was visible for 35 minutes. A 90% confidence limit on bursts from Relay 2 is therefore once per 15–350 minutes, and a limit of once per 44–1000 days for such bursts from all spacecraft visible to ASKAP.

3.1. Electrostatic discharge from a current arc

Spacecraft primarily charge through the accumulation of electrons through interactions with plasma in the space environment (James et al. 1994). When sufficient voltage is achieved, electrostatic discharge (ESD) occurs, typically between nearby surfaces/materials on the spacecraft. ESD does not depend on the operational nature of the spacecraft, so ESD from a satellite decommissioned 60 yr ago is entirely plausible.

It has long been known that ESD causes radio frequency pulses. This has been studied in laboratory conditions

¹ <https://rhodesmill.org/skyfield/>

² <https://www.n2yo.com/satellite/?s=737>

³ <https://nssdc.gsfc.nasa.gov/nmc/spacecraft/displayTrajectory.action?id=1964-003A>

⁴ https://en.wikipedia.org/wiki/Zombie_satellite

(Leung 1985, available at <https://ntrs.nasa.gov/citations/19860010269>), and through sensors mounted on spacecraft (e.g. Guidice et al. 1992). Most similarly to our burst detection, Ferguson et al. (2017) performed an observational campaign using the Arecibo ground-based radio telescope. Measurements made in the 300–350 MHz band detected a large number of impulsive bursts from a beam centred on a GPS satellite, with the greatest having a peak flux density corresponding to 3000 Jy. The observed arcing was attributed to charging and breakdown of the 1.5 m solar array on the satellites, and the arcing rate (coupled to the expected damage per arcing event) was consistent with the long-term power degradation rate observed for these arrays.

The bursts seen by Ferguson et al. (2017) have key similarities with our event. Given the greater distance to a GPS orbit of approximately 20,000 km, the expected flux density had the satellite been at a distance of 4300 km would have been 65 kJy — significantly less than what we observe. However, as a very early spacecraft, Relay 2 may have been constructed from materials with higher resistivities capable of holding greater charge and hence producing stronger ESD events (Garrett & Whittlesey 2012). Furthermore, the pulse shape plotted in Figure 7 of their work exhibits a similar secondary peak of magnitude $\sim 25\%$ of the peak power. However, the typical observed burst duration for Arecibo bursts was 40–50 μs , i.e. at least 1000 times longer than our burst. A detailed analysis of arcing from photovoltaic cells in laboratory experiments with 0.5 ns resolution by Ferguson et al. (2022) reveals arc currents varying at rates of up to 200 MHz, but the currents undergo many oscillations, and do not produce a single spike of emission. The typical rise-time of arcing currents from dielectric plates to conductive substrates is approximately 3 ns, with a total duration of 10 ns, and would thus be capable of producing the observed emission, though other materials also experience extremely short rise-times (Jet Propulsion Laboratory 1999). While the above analyses do not examine the polarisation signature, it is expected that arcing produces polarisation in the observer–current plane (Damas & Robiscoe 1988). A linear current would then produce linear polarisation.

We can find no specific trigger for such an ESD. Relay 2’s orbit passes through the inner Van Allen belt, though at the time of the burst, it was at a significantly lower altitude. While the Sun was near the peak of the solar cycle, it was unusually inactive, with a global K_p index of 1 at the time of the event (Matzka et al. 2021, available at <https://kp.gfz-potsdam.de/en/>), so that anomalously high charging due to geomagnetic activity can be excluded. Hence, such bursts from Relay 2 may be a regular occurrence under normal conditions.

3.2. A micrometeoroid impact scenario

It is also possible that the burst was triggered by a micrometeoroid impact, which can result in charging events due to the plasma cloud generated upon impact, or discharge due to this plasma increasing the conductivity of the space environment (Garrett & Close 2013). Micrometeoroid impacts can also produce direct radio-frequency emission. Laboratory experiments simulating these impacts on a variety of materials (at typically less than 10 km s^{-1}) have detected pulses lasting 2 ns (Maki et al. 2005), with the suggested emission mechanism being due to discharge over the cracks produced in a material from the impact. These pulses were found to occur in groups however, with individual pulses separated by 17 ns to 40 μs . Li et al. (2023) found qualitatively similar behaviour, with emission being strongest at a very low frequency of 1 kHz, but with a significant frequency peak at 10 MHz. However, very narrow spikes ($\ll 100 \text{ ns}$) in the time domain were also present, suggesting that higher-frequency emission, perhaps up to the ASKAP observation band, is also possible.

Fletcher (2015) have performed smooth-particle hydrodynamics simulations of impacts up to 72 km s^{-1} , finding field strengths of 10 V/m at 40 cm distance for a 1 ng ($4.6 \mu\text{m}$) impactor travelling at 20 km s^{-1} . The field was predominantly in a single direction, implying that linearly polarised emission would be produced. The author notes that this emission is direct emission from the plasma, which is produced for impacts above approximately 18 km s^{-1} when the plasma is fully ionised, and that the peak electric field strength tends to saturate at higher velocities/impactor masses. However, if the linear dimensions of the plasma cloud scale with the cube root of the impactor mass, the far-field strength will also scale proportionally, so that a 22 μg micrometeoroid could produce the observed field strength for our burst. Estimates of the micrometeoroid flux give a rate of $2 \cdot 10^{-9} \text{ m}^{-2} \text{ s}^{-1}$ above this mass (Maki et al. 2005). Assuming an average of one satellite with 1 m^2 cross-section in ASKAP’s field of view at any given moment (at a characteristic distance of 1000 km, ASKAP’s 30 deg^2 FOV covers an area of approximately $10,000 \text{ km}^2$, giving 0.2 satellites per FOV when compared to $\mathcal{O} \sim 10^4$ satellites spread over $4\pi R_E^2 \sim 5 \cdot 10^8 \text{ km}^2$ for an Earth radius of $R_E = 6,378 \text{ km}$), this translates to a probability of 1.7% in the 100.5 days of CRACO observation.

We therefore consider emission from a micrometeoroid impact to be a plausible explanation for the burst, but favour the ESD scenario due to similarities with ESD events observed with Arecibo, and because ESD may be more likely from an older satellite. We note that neither emission mechanism explains the two circularly polarised frequency bands shown in Figure 3.

4. Implications

Nanosecond-scale radio impulses are commonly studied in other applications. In particular, experiments measuring radio emission from high-energy particle cascades search for impulsive signals of 1–100 ns duration (Schröder 2017), and regularly encounter RFI on these timescales. This makes bursts (be they due to ESD or micrometeoroid impacts) a potential impostor signal for experiments looking for radio-emission from high-energy particles. Conversely, such astroparticle experiments could readily be made capable of detecting space-borne impulsive radio-frequency events. Cosmic ray searches with the Low Frequency Array (LOFAR; Schellart et al. 2013), and the Auger Engineering Radio Array (AERA; The Pierre Auger Collaboration 2016), operate in the 10–100 MHz range on nanosecond timescales, and should be able to identify such events.

In addition to ASKAP, there are a large number of experiments operating in the 400 MHz–1.5 GHz range that search for fast radio bursts on $\mathcal{O} \sim$ ms timescales (e.g. Jankowski et al. 2023; CHIME/FRB Collaboration et al. 2021; Law et al. 2023), many of which have relatively large fields of view that regularly observe satellites coincidentally. In particular, instruments designed for the all-sky monitoring of FRBs at GHz frequencies (e.g. Connor et al. 2021; Luo et al. 2024) could, if appropriately retrofitted, be ideal for detecting such events.

5. Conclusion

We have observed a 30 ns burst of 695.5 MHz–1031.5 MHz radio emission from the non-operational Relay 2 satellite. Our ability to resolve the peak of the burst, which we estimate to be < 3 ns duration and > 3 MJy, is limited by the dynamic range of the ASKAP/CRACO system. We suggest that the burst originated from an electrostatic discharge (ESD) event, or potentially a micrometeoroid impact, and consider that such events may be relatively common. The burst properties are consistent with those previously observed from a GPS satellite, but on a 1000 times shorter timescale. The observation of such a short burst at GHz frequencies is unexpected, and raises the prospect of new methods of remote sensing of arc discharges from satellites, either from retrofitting existing experiments searching for fast radio bursts or high-energy particles, or new dedicated instruments.

Acknowledgements

This work uses data obtained from Inyarrimanha Ilgari Bundara / the CSIRO Murchison Radio-astronomy Observatory. We acknowledge the Wajarri Yamaji People as the Traditional Owners and native title holders of the Observatory site. CSIRO’s ASKAP radio telescope is part of the Australia Telescope National Facility (<https://ror.org/05qajvd42>). Operation of ASKAP is funded by the Australian Government with support from the National Collaborative Research Infrastructure Strategy. ASKAP uses the resources of the Pawsey Supercomputing Research Centre. Establishment of ASKAP, Inyarrimanha Ilgari Bundara, the CSIRO Murchison Radio-astronomy Observatory and the Pawsey Supercomputing Research Centre are initiatives of the Australian Government, with support from the Government of Western Australia and the Science and Industry Endowment Fund.

CRACO was funded through Australian Research Council Linkage Infrastructure Equipment, and Facilities grant LE210100107.

Part of this work was performed on the OzSTAR national facility at Swinburne University of Technology. The OzSTAR program receives funding in part from the Astronomy National Collaborative Research Infrastructure Strategy (NCRIS) allocation provided by the Australian Government, and from the Victorian Higher Education State Investment Fund (VHESIF) provided by the Victorian Government.

RMS acknowledges support through ARC Future Fellowship FT190100155 and Discovery Project DP220102305. ATD and JJ-S acknowledges support through Australian Research Council Discovery Project DP220102305. MG is supported by the Australian Government through the Australian Research Council’s Discovery Projects funding scheme (DP210102103), and through UK STFC Grant ST/Y001117/1. MG acknowledges support from the Inter-University Institute for Data Intensive Astronomy (IDIA). IDIA is a partnership of the University of Cape Town, the University of Pretoria and the University of the Western Cape. For the purpose of open access, the author has applied a Creative Commons Attribution (CC BY) licence to any Author Accepted Manuscript version arising from this submission.

Facilities: ASKAP

Software: NUMPY 2.2.1 (van der Walt et al. 2011), SCIPY 1.15.0 (Virtanen et al. 2020), ASTROPY 7.0.0

REFERENCES

Allen, J. 2010, *Space Weather*, 8, S06008,
doi: 10.1029/2010SW000588

CHIME/FRB Collaboration, Amiri, M., Andersen, B. C., et al. 2021, *ApJS*, 257, 59, doi: 10.3847/1538-4365/ac33ab

- Connor, L., Shila, K. A., Kulkarni, S. R., et al. 2021, *PASP*, 133, 075001, doi: [10.1088/1538-3873/ac0bcc](https://doi.org/10.1088/1538-3873/ac0bcc)
- Damas, M. C., & Robiscoe, R. T. 1988, *Journal of Applied Physics*, 64, 566, doi: [10.1063/1.341971](https://doi.org/10.1063/1.341971)
- DeForest, S. E. 1972, *J. Geophys. Res.*, 77, 651, doi: [10.1029/JA077i004p00651](https://doi.org/10.1029/JA077i004p00651)
- Ferguson, D., Crabtree, P., White, S., & Vayner, B. 2016, *Journal of Spacecraft and Rockets*, 53, 464, doi: <https://doi.org/10.2514/1.A33438>
- Ferguson, D., White, S., Rast, R., et al. 2017, *Journal of Spacecraft and Rockets*, 54, 566, doi: [10.2514/1.A33724](https://doi.org/10.2514/1.A33724)
- Ferguson, D. C., Murray-Krezan, J., Barton, D. A., Dennison, J. R., & Gregory, S. A. 2014, *Journal of Spacecraft and Rockets*, 51, 1907, doi: [10.2514/1.A32958](https://doi.org/10.2514/1.A32958)
- Ferguson, D. C., Perillat, P., & Vayner, B. 2022, *Journal of the Astronautical Sciences*, 69, 139, doi: [10.1007/s40295-021-00295-8](https://doi.org/10.1007/s40295-021-00295-8)
- Fletcher, A. 2015, PhD thesis, Stanford University, Department of Aeronautics and Astronautics
- Garrett, H. B., & Whittlesey, A. C. 2012, *Guide to Mitigating Spacecraft Charging Effects* (John Wiley & Sons, Ltd), doi: <https://doi.org/10.1002/9781118241400.ch1>
- Garrett, H. B., & Close, S. 2013, *IEEE Transactions on Plasma Science*, 41, 3545, doi: [10.1109/TPS.2013.2286181](https://doi.org/10.1109/TPS.2013.2286181)
- Goddard Space Flight Centre. 1965, Final Report on the Relay I Program. NASA SP-76, Vol. 76 (National Aeronautics and Space Administration). <https://ntrs.nasa.gov/api/citations/19660000937/downloads/19660000937.pdf>
- Greisen, E. W. 2003, in *Astrophysics and Space Science Library*, Vol. 285, *Information Handling in Astronomy - Historical Vistas*, ed. A. Heck, 109, doi: [10.1007/0-306-48080-8_7](https://doi.org/10.1007/0-306-48080-8_7)
- Guidice, D. A., Davis, V. A., Curtis, H. B., et al. 1992, in *NASA Conference Publication*, Vol. 3127, *Fifth Annual Workshop on Space Operations Applications and Research (SOAR 1991)*, ed. K. Krishen, 662
- Hotan, A. W., Bunton, J. D., Chippendale, A. P., et al. 2021, *PASA*, 38, e009, doi: [10.1017/pasa.2021.1](https://doi.org/10.1017/pasa.2021.1)
- James, B. F., Norton, O., & Alexander, M. B. 1994, *The Natural Space Environment: Effects on Spacecraft*, Vol. NASA Reference Publication 1350 (National Aeronautics and Space Administration). <https://ntrs.nasa.gov/api/citations/19950019455/downloads/19950019455.pdf>
- Jankowski, F., Bezuidenhout, M. C., Caleb, M., et al. 2023, arXiv e-prints, arXiv:2302.10107, doi: [10.48550/arXiv.2302.10107](https://doi.org/10.48550/arXiv.2302.10107)
- Jet Propulsion Laboratory. 1999, *Electrostatics discharge (ESD) test practices*, Tech. Rep. PRACTICE NO. PT-TE-1414, National Aeronautics and Space Administration. <https://llis.nasa.gov/lesson/777>
- Law, C. J., Sharma, K., Ravi, V., et al. 2023, arXiv e-prints, arXiv:2307.03344, doi: [10.48550/arXiv.2307.03344](https://doi.org/10.48550/arXiv.2307.03344)
- Leach, R. D., & Alexander, M. B. 1995, *Failures and anomalies attributed to spacecraft charging*
- Leung, P. 1985, *Characterization of EMI generated by the discharge of a VOLT solar array*, Final Report Jet Propulsion Lab., California Inst. of Tech., Pasadena.
- Li, H., Zhang, L., Han, J., Cai, M., & Tao, M. 2023, *International Journal of Impact Engineering*, 178, 104619, doi: <https://doi.org/10.1016/j.ijimpeng.2023.104619>
- Luo, R., Ekers, R., Hobbs, G., et al. 2024, *PASA*, 41, e109, doi: [10.1017/pasa.2024.108](https://doi.org/10.1017/pasa.2024.108)
- Maki, K., Soma, E., Takano, T., Fujiwara, A., & Yamori, A. 2005, *Journal of Applied Physics*, 97, 104911, doi: [10.1063/1.1896092](https://doi.org/10.1063/1.1896092)
- Matzka, J., Stolle, C., Yamazaki, Y., Bronkalla, O., & Morschhauser, A. 2021, *Space Weather*, 19, e2020SW002641, doi: [10.1029/2020SW002641](https://doi.org/10.1029/2020SW002641)
- NASA Historical Staff, Office of Policy Analysis. 1966, *Astronautics and Aeronautics, 1965: Chronology on Science Technology, and Policy*. NASA SP-4006, Vol. 4006 (National Aeronautics and Space Administration). <https://www.nasa.gov/wp-content/uploads/2023/04/1965.pdf?emrc=ee9c46>
- Schellart, P., Nelles, A., Buitink, S., et al. 2013, *A&A*, 560, A98, doi: [10.1051/0004-6361/201322683](https://doi.org/10.1051/0004-6361/201322683)
- Schröder, F. G. 2017, *Progress in Particle and Nuclear Physics*, 93, 1, doi: [10.1016/j.pnpnp.2016.12.002](https://doi.org/10.1016/j.pnpnp.2016.12.002)
- Scott, D. R., Cho, H., Day, C. K., et al. 2023, *Astronomy and Computing*, 44, 100724, doi: [10.1016/j.ascom.2023.100724](https://doi.org/10.1016/j.ascom.2023.100724)
- Shannon, R. M., Bannister, K. W., Bera, A., et al. 2024, arXiv e-prints, arXiv:2408.02083, doi: [10.48550/arXiv.2408.02083](https://doi.org/10.48550/arXiv.2408.02083)
- Sotomayor-Beltran, C., Sobey, C., Hessels, J. W. T., et al. 2013, *A&A*, 552, A58, doi: [10.1051/0004-6361/201220728](https://doi.org/10.1051/0004-6361/201220728)
- Sutinjo, A. T., Scott, D. R., James, C. W., et al. 2023, *ApJ*, 954, 37, doi: [10.3847/1538-4357/ace774](https://doi.org/10.3847/1538-4357/ace774)
- The Pierre Auger Collaboration. 2016, *Journal of Instrumentation*, 11, P01018, doi: [10.1088/1748-0221/11/01/P01018](https://doi.org/10.1088/1748-0221/11/01/P01018)
- van der Walt, S., Colbert, S. C., & Varoquaux, G. 2011, *Computing in Science and Engineering*, 13, 22, doi: [10.1109/MCSE.2011.37](https://doi.org/10.1109/MCSE.2011.37)
- Virtanen, P., et al. 2020, *Nature Methods*, 17, 261, doi: [10.1038/s41592-019-0686-2](https://doi.org/10.1038/s41592-019-0686-2)
- Wang, Z., Bannister, K. W., Gupta, V., et al. 2024, arXiv e-prints, arXiv:2409.10316, doi: [10.48550/arXiv.2409.10316](https://doi.org/10.48550/arXiv.2409.10316)